Available online at www.sciencedirect.com
SCIENCE DIRECT®
Journal of Sound and Vibration 278 (2004) 155–179
JOURNAL OF SOUND AND VIBRATION
www.elsevier.com/locate/jsvi

Aeroacoustic features of coupled twin jets with spanwise oblique shock-cells

Praveen Panickar, K Srinivasan[1], Ganesh Raman*

Fluid Dynamics Research Center, Illinois Institute of Technology, 10 West 32nd Street, Chicago, IL 60616, USA

Received 12 March 2003; accepted 1 October 2003

Abstract

This paper experimentally investigates the aeroacoustics of coupled twin jets of complex geometry. The study was motivated by the fact that twin jet configurations that are commonly used in aircraft propulsion systems can undergo unpredictable resonant coupling resulting in structural damage. Further, nozzles with spanwise oblique exits are increasingly being considered for their aerodynamic and acoustic advantages, as well as stealth benefits. Although several studies have examined aspects of twin jet coupling, very little data is available on the coupling of jets from nozzles of complex geometry. Our study focuses on twin convergent nozzles with an aspect ratio of 7 with spanwise oblique exits operated over the fully expanded Mach number range from 1.3 to 1.6. The inter-nozzle spacing (s/h) was varied from 7.4 to 13.5. However, the focus remained on the lower spacing that is more representative of aircraft applications. Several interesting results have emerged from this study: (1) Coupling of twin nozzles with a beveled exit was observed only when the beveled edges faced each other and the nozzles formed a 'V' shape in the inter-nozzle region. Specifically, if the two beveled edges were oriented away from each other to form an arrowhead ('A') shape no coupling was observed. (2) Despite the presence of spanwise antisymmetric, spanwise symmetric and spanwise oblique modes for the single nozzles, only the first two modes were evident in the coupling. (3) The symmetric coupling produced unsteady pressures in the inter-nozzle region that were up to 7.5 dB higher than the antisymmetrically coupled case. (4) Dynamic tests conducted by moving the nozzles apart while they were operating or by continuously changing the stagnation pressure at fixed inter-nozzle spacing revealed that coupling modes could co-exist at non-harmonically related frequencies. These dynamic tests reproduced the static test data. (5) The frequency of both coupling modes agrees with the higher order waveguide modes based on Tam's theory. (6) Differences in broadband shock noise between the 'V' and 'A' configurations were also documented. Our results provide an understanding of complex twin jet coupling and will serve as benchmark data for validating computational models.

*Corresponding author. Tel.: +1-312-567-3554; fax: +1-312-567-3173.
E-mail address: raman@iit.edu (G. Raman).
[1] Present address: Indian Institute of Technology, Guwahati, India.

0022-460X/$ - see front matter © 2003 Elsevier Ltd. All rights reserved.
doi:10.1016/j.jsv.2003.10.011

1. Introduction

Most supersonic jet aircraft exhaust systems are imperfectly expanded in flight which places an emphasis on the components of shock noise. Shock noise has two main components—the broadband component and a discrete tone. This discrete tone component is called screech. Screech, discovered by Powell [1], is caused by a feedback loop that involves the interaction of the hydrodynamic disturbances with the shock. This interaction leads to the production of pressure waves that propagate to the nozzle exit and couple with nascent hydrodynamic disturbances, thus completing the feedback loop. Raman [2] recently summarized half a century of research on screech.

The presence of screech components in underexpanded jets can cause nozzle or tail plane damage. In aircraft with twin closely spaced nozzles, the jet plumes can couple and lead to even higher dynamic pressures in the inter-nozzle region. These pressures may cause significant structural damage to the nozzle material and may also cause fatigue failure of the material. In some cases the high dynamic pressures may also cause damage to the advanced materials used on aircraft bodies (stealth paint or aircraft skin). Twin nozzles of complex geometry—particularly double beveled in the case of the new F-22s—have found special use in modern aircraft because of their variable area and aspect ratio, and thrust vectoring capabilities. The proper functioning of such beveled nozzles under adverse conditions is of concern.

1.1. Review of relevant literature

Most of the published works on twin jets have focused on jets having circular exit geometry. Berndt [3] performed a series of wind tunnel experiments to measure the dynamic pressure fluctuations on the nozzle surfaces of a twin jet nacelle and was able to conclude that the pattern of the highest dynamic pressures measured in the wind tunnel matched the pattern of the hardware damage that occurred during the flight test program. Seiner et al., [4] experimentally showed that for closely spaced supersonic jets operating at off design conditions, the dynamic pressures upstream of the jet exits can reach levels that could result in structural damage. Tam and Seiner [5] observed that the twin jet screech frequency was greater than the frequency of two jets that did not interact with each other. Morris [6] showed how an instability wave analysis could provide some insight into the interaction of twin supersonic circular jets. His analysis showed how the growth rates of instability waves or large structures in the initial mixing region of the twin jets are affected by the jet separation. Wlezien [7] showed that the noise produced by the mutual interaction of two supersonic plumes is a strong function of nozzle spacing and the fully expanded jet Mach number. Shaw [8] examined methods to evaluate the effectiveness of several concepts in suppressing the twin jet screech i.e., tabs, lateral spacing, axial spacing and secondary jets.

Compared to the information available for circular jets, there is a very limited amount of data available on jets with rectangular exit geometry. Moreover, of late, the focus has shifted to scarfed [9], asymmetric [10], beveled [11–13], and trailing edge modified [14,15] nozzles. Raman and Taghavi [16] also studied the flow and acoustic features of multiple supersonic uniform exit rectangular jets with phase locked screech. Later, Raman and Taghavi [17] conducted a detailed study of the near acoustic field and the coupling mechanism of twin rectangular supersonic jets having uniform exit geometry. They found that there were two modes of coupling that

prevailed—the symmetric mode that augmented the screech amplitude and the antisymmetric mode that suppressed it and both these modes were mutually exclusive. A companion study by Taghavi and Raman [18] on twin jets having straight rectangular exit geometry in various configurations found that the shock spacing did not change significantly when the jets coupled.

The coupling of twin supersonic jets of double beveled exit geometry was studied by Raman [19], and it was found that twin double beveled jets can couple and may lead to either an augmentation or suppression of sound in the inter-nozzle region depending on the fully expanded Mach number at which the jets were operating. Although previous work has illuminated some aspects of individual single beveled nozzles [20,21], to the best of our knowledge there is no published information on the interaction of twin supersonic jets having single beveled exit geometry. In addition, the effect of varying nozzle separation while the nozzles were operating appears never to have been considered before. Note that the rectangular shock containing jets exhibit both spanwise and transverse oscillation modes. For high aspect ratio ($b/h > 5$) nozzles, the transverse oscillation mode is predominantly antisymmetric. However in the spanwise direction symmetric, antisymmetric and oblique oscillation modes are possible. Greater detail regarding spanwise modes is provided in Section 3.1.

1.2. Objectives

The main focus of this research is the study of twin nozzles of spanwise oblique geometry. A bevel angle of 30° was chosen due to a wealth of information in the literature on single nozzles at this angle. The schematic diagrams of the configurations studied in this paper are shown in Fig. 1. Underexpanded single beveled nozzles can produce screech noise in spanwise oblique modes. It is presumed that the spanwise oblique modes of screech noise are caused by the spanwise oblique shock cells, revealed in the schlieren images taken from Raman [21] and reproduced in Fig. 2.

The specific objectives of the present study are:

- To examine the spanwise behavior of single-beveled rectangular jets in single jet and twin jet configurations ('A' and 'V' as shown in Fig. 1) and to identify the screech modes (symmetric or antisymmetric) produced by twin jets from spanwise oblique nozzles using detailed steady and unsteady measurements in the near field.
- To study the behavior of twin jets under dynamically varying conditions, namely inter-nozzle spacing and stagnation pressure, using continuous instantaneous spectra.
- To report the various manifestations of coupling, revealed by phase averaged measurements, and acoustic pressure distribution in the inter-nozzle region. Phase averaged measurements provide an insight into the dynamic pressure loads which is more relevant to the problem at hand rather than the mean sound pressure levels.
- To examine the applicability of Tam's waveguide theory to single and twin coupled jets from beveled geometries.
- To survey the directivity of sound pressure along the central vertical plane of the two twin jet configurations (namely, the V-shaped configuration and the arrowhead shaped (A) configuration).
- To study the differences in broadband noise emission between the two twin jet configurations.

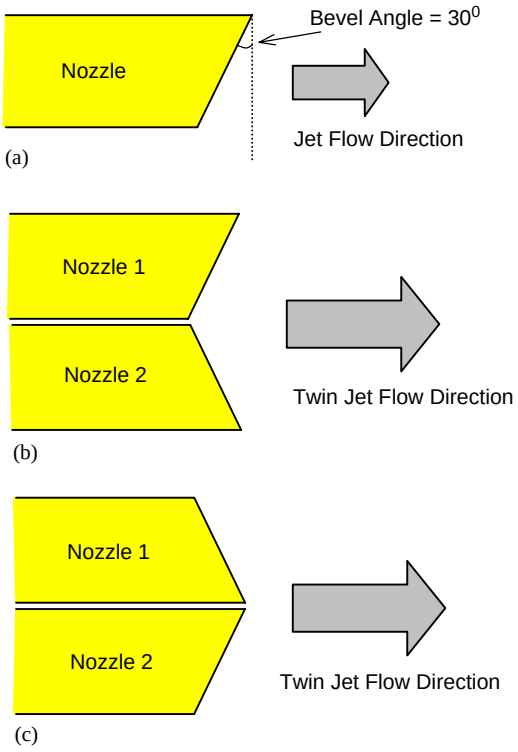

Fig. 1. Schematic diagrams showing single and twin jet configurations: (a) single jet, (b) twin jet: V-shaped configuration, (c) twin jet: arrowhead-shaped configuration.

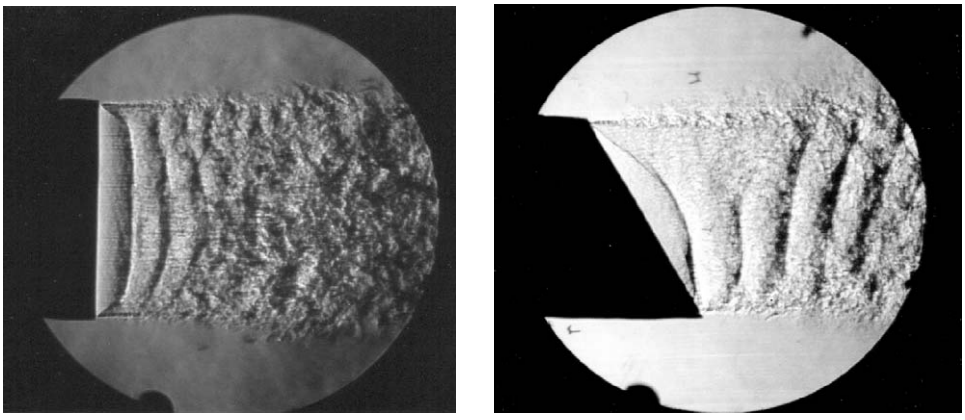

Fig. 2. Spark-schlieren photographs comparing shock containing jets from uniform and spanwise beveled nozzles from Raman [21]: (a) uniform exit, (b) single beveled exit. Note the spanwise oblique shock cell structure.

2. Experimental apparatus and procedure

The experiments were carried out in the high-speed jet facility at the Fluid Dynamics Research Center, Illinois Institute of Technology, Chicago. This facility receives compressed air at a maximum initial pressure of approximately 1.54 MPa from storage tanks that have a total volume of approximately 198 m^3. The compressor bank is made of three compressors and serves not only to charge the storage tanks before a run but also to extend the life of each run by supplementing their flow incrementally as the pressure falls during blow down. The settling chamber has walls covered with acoustic foam in order to reduce flow borne acoustic disturbances. Furthermore, honeycomb sections and screens provide additional flow conditioning. The compressed air system can provide a maximum momentary exit pressure ratio of 15.3 resulting in a fully expanded Mach number of 2.4 and a Reynolds number based on exit diameter of 5.4×10^6 based on an exit diameter of 25.4 mm. The jet exhausts into an anechoic chamber, equipped with multiple access panels including a set of optical windows. The jet nozzles are connected to the stagnation chamber by means of reinforced flexible tubing to facilitate positioning of the nozzles, during dynamic tests, as well as to enable a quick transition between different configurations. The nozzles are mounted on an uni-axial traverse, with the lead screw having opposite threads for each nozzle. Thus, the motorized traverse can move the nozzles towards, or away from each other. The nozzle axes are kept parallel to each other for all the experiments described in this study. While this does not necessarily depict actual aircraft operating conditions, it provides a baseline where the coupling studies could begin. Further results with different axial orientations will be discussed in a forthcoming paper. The spanwise width of each nozzle was 33.58 mm and the transverse dimension was 5.08 mm, which meant that the nozzles used had an aspect ratio of about 7. Zilz and Wlezien [22] showed that for low aspect ratio jets it was possible to have oscillation modes in the spanwise as well as the transverse directions. For large aspect ratio jets, such as the ones used in this study, the transverse oscillation modes are predominantly antisymmetric and the spanwise modes can vary. The lip thickness of the nozzles was 2.0 mm which meant that at the closest location the inter-nozzle separation parameter $s/h = 7.4$. The nozzles were tested in the fully expanded jet Mach number range from 1.28 to 1.6. The Mach number range studied is narrow since the jets did not screech in the twin jet configuration beyond this range.

All acoustic measurements were made using 6.35 mm diameter B & K microphones. The microphones were calibrated using a B & K pistonphone calibrator. The sound pressure levels reported are in dB relative to 20 μPa. All the data acquisition was achieved using a PC-based National Instruments data acquisition board capable of acquiring 1.6 Megasamples/s, using Labview 6. Spectra were obtained by sampling at 200 kHz, dividing the time series into 50 records and taking FFT blocks of 4096 data points each. Phase data was processed using the Matlab software.

2.1. Uncertainty of measurements

The uncertainty in the SPL measurements could be attributed to three sources, namely, the uncertainty in the fluctuating pressure data acquired by the microphone, the uncertainty due to number of records averaged for obtaining the FFT, and the uncertainty in the stagnation pressure measurements. Of all these three sources the uncertainty in the stagnation pressure measurements

by the pressure transducer played the most dominant role. The uncertainty in the SPL measurements is calculated to be 1%, including repeatability factors. The error in the frequency measurements was within 2%. The fully expanded Mach number for each of the data points was obtained by considering an isentropic expansion of the jet to atmospheric conditions. Hence the uncertainty in the fully expanded Mach number value is calculated to be 0.016%. Error bars are shown on key figures. The dynamic tests performed also showed good repeatability.

3. Results and discussion

3.1. Twin jet coupling modes

Before beginning to examine the data to obtain the spanwise modes, a brief definition of the spanwise modes that could be expected is presented in the following list:

1. Phase locked operation of the twin jets with the spanwise phase angle approximately 0° corresponds to a spanwise symmetric mode.
2. Phase locked operation of the twin jets with the spanwise phase angle approximately 180° corresponds to a spanwise antisymmetric mode.
3. Phase locked operation of the twin jets with the spanwise phase angle between 0° and 180° corresponds to a spanwise oblique mode.
4. Non phase locked operation (which in this case means that the frequencies recorded by the individual microphones are different).

The jet modes were examined by mounting microphones at the two spanwise extreme ends of the nozzle in the case of the single jet, and at the respective nozzle centers in the case of the twin jets, and in both cases, slightly upstream of the nozzle lip. This was done in order to investigate the characteristics of the outer cycle of the screech loop. However, previous work that recorded phase conditioned schlieren and microphone data simultaneously (Raman and Taghavi [17]), showed a clear correspondence between the phase measurements made by the microphone and the motions within the jet plume. The single beveled jets used in this study screeched in the audible range when operated individually. The parameters used in the present investigation are Mach number, and the inter-nozzle (center-to-center) spacing, 's' non-dimensionalized using the shorter nozzle dimension 'h' (see Fig. 4). In the case of twin jets, at least two geometric configurations are possible, one in which the bevel planes of the individual nozzles faced each other, which is being referred to as "*V-shaped*" configuration (Fig. 1(b)), and another in which the bevel planes do not face each other, which is referred as "*Arrowhead-shaped*" ('A') configuration (Fig. 1(c)). For the present study, we define coupling as follows: when two individual jets having slightly different frequencies are placed next to each other they are said to couple if their interaction produces a single frequency accompanied by the phase locking of the screech instabilities of the two jets.

Fig. 3 shows the schematic arrangement for the arrowhead-shaped ('A') configuration (Fig. 3(a)), and a plot of the relative phase difference between the spanwise microphones (Fig. 3(b)). The inter-nozzle spacing for this plot was $s/h = 7.4$. As can be seen from Fig. 3(b), a wide variation in the phase difference exists between the two jets, across the entire Mach number range covered in the present study. This indicates the absence of phase locked coupling between

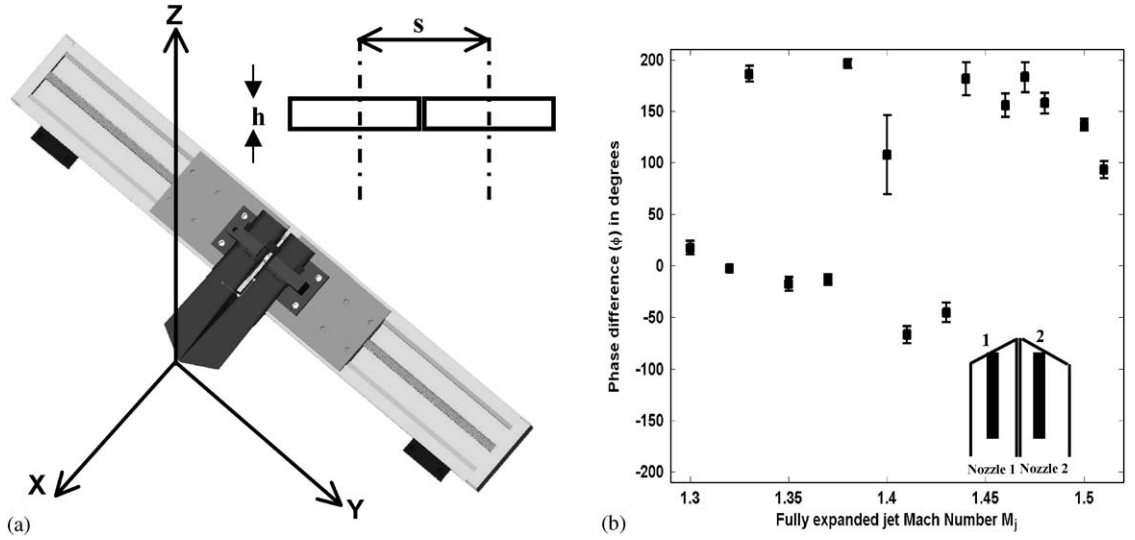

Fig. 3. Twin jet in the arrowhead or A-shaped configuration and spanwise phase associated with it. (a) A-shaped twin jet configuration of the two single beveled nozzles, along with the co-ordinate axis setup, and nozzle dimension nomenclature used during the experimental study. (b) Spanwise phase angle between the two jets as measured by microphones 1 and 2. The microphone locations are on the spanwise center of the individual nozzle as shown by the black rectangular strips in the schematic. This configuration showed no coupling as is evident from the phase chart.

the individual jets, establishing that the single beveled nozzles do not couple in the arrowhead-shaped ('A') configuration.

In contrast, the V-shaped configuration (Fig. 4(a)) exhibits coupling behavior as shown in Fig 4(b). In this plot, the inter-nozzle spacing was $s/h = 7.4$. It is clear from Fig. 4(b) that the coupling is symmetric (phase difference ≈ 0) at the lower Mach numbers and antisymmetric (phase difference $\approx 180^\circ$) at the mid-range and higher Mach numbers covered in this study. It was observed that there was an abrupt change of phase from 0° to 180° at a fully expanded Mach number of 1.4. After this point the phase remains antisymmetric throughout the entire Mach number range. The result here is in sharp contrast to that found by Raman and Taghavi [17] who found that for twin rectangular jets with uniform exits the jets coupled in the antisymmetric mode at low Mach numbers and in the symmetric mode at higher Mach numbers. The frequencies recorded by the individual microphones for both the twin jet configurations are given in Table 1. This table shows that the jets are frequency locked in the V-shaped configuration, whereas the screech frequencies are distinctly different for the arrowhead-shaped configuration.

The above observations raise the question of why one configuration couples and the other does not. It is interesting to note that Raman [19] studied double beveled jets in single and twin configurations and found that these jets exhibit both, spanwise symmetric and spanwise antisymmetric, modes even when operated individually. The arrowhead-shaped configuration is similar to an individual double beveled jet with a splitter plate inserted along the flow direction along the spanwise center. It may be reasoned that the V-shaped configuration offers a larger interaction region than in the case of the arrowhead-shaped configuration. In the V-shaped configuration, all points on a nozzle exit are in line-of sight with the corresponding point on its

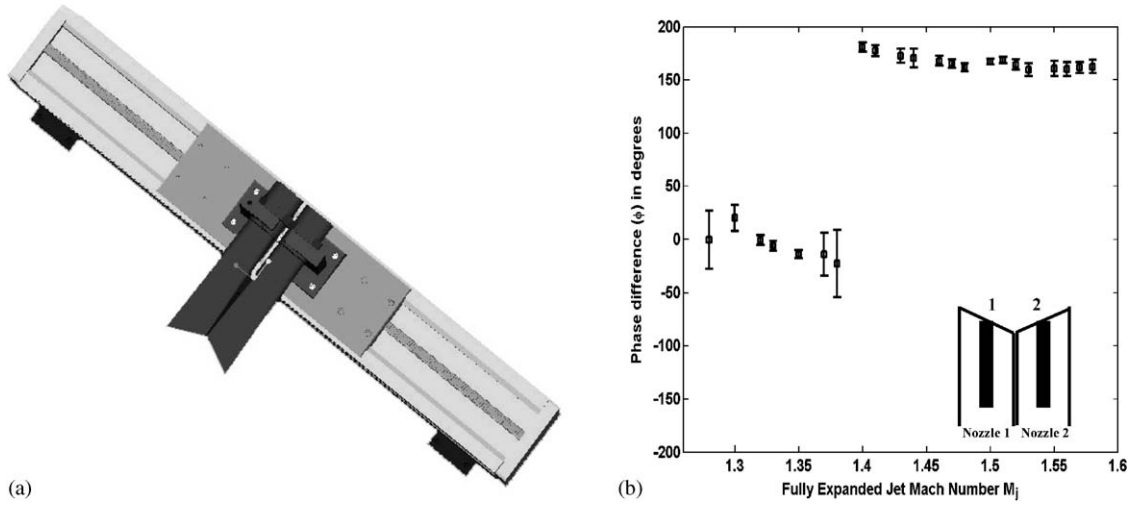

Fig. 4. Twin jet in the V-shaped configuration and spanwise phase associated with it. (a) Schematic of V-shaped configuration of the two single beveled nozzles. (b) Spanwise phase angle between the two jets as measured by microphones 1 and 2. The microphone locations are on the spanwise center of the individual nozzle as shown by the black rectangular strips in the schematic.

Table 1
Table showing spanwise frequencies for the configurations shown in Figs. 3(a) and 4(a). Microphone positions as indicated in Figs. 3(b) and 4(b). For phase locked coupling we would expect the exact same frequency to be recorded by both the microphones which is not observed for the configuration in Fig. 3(a), indicating the absence of phase locked coupling

Mach number (M_j)	Configuration in Fig. 3(a)		Configuration in Fig. 4(a)	
	Microphone 1 frequency (Hz)	Microphone 2 frequency (Hz)	Microphone 1 frequency (Hz)	Microphone 2 frequency (Hz)
1.30	15,332	15,186	15,527	15,527
1.35	13,818	13,672	14,648	14,648
1.38	12,939	12,988	13,770	13,770
1.41	12,402	12,256	12,451	12,451
1.46	11,426	11,328	11,523	11,523
1.47	11,230	11,084	11,279	11,279
1.50	10,644	10,596	10,889	10,889

neighboring nozzle, whereas, this is not true for the arrowhead configuration, where only the points on the downstream edge of the nozzles see each other. Although there is no information in the literature connecting spanwise flow communication with coupling it appears that a larger interaction region encourages jet coupling. The mechanism behind this phenomenon warrants a deeper study of the physics of the flow and is, as yet, an unresolved issue and beyond the scope of this study. In addition some clues are provided by the work of Rice and Raman [12] who showed that for convergent single beveled nozzles with a 30° bevel the flow field of the jet was deflected on account of the spanwise pressure relief. Thus in the V-shaped configuration the jets would be

deflected towards each other whereas in the A-shaped configuration they would deflected away from each other resulting in a reduced propensity to couple. The fact that the arrowhead-shaped configuration showed no spanwise symmetric or antisymmetric modes may prove to be useful in the design of nozzles having oblique geometries to be used in single or twin configuration. Note that all discussions pertaining to coupling are made only with reference to the V-shaped configuration that coupled.

The characteristics of each individual nozzle were also studied separately. The single beveled nozzle was tested and the phase difference across the spanwise direction was measured and it was found that the spanwise phase for the individual single beveled nozzle could be antisymmetric, symmetric or oblique. Both single beveled nozzles exhibited a spanwise antisymmetric mode at the lower Mach numbers from 1.28 to 1.38 and a spanwise oblique mode at the higher Mach numbers 1.48–1.58. One of the jets also exhibited a spanwise symmetric mode at the midrange Mach numbers from 1.4 to 1.46 and in this Mach number range the other jet exhibited spanwise oblique modes. In other words, the individual jets screech in well defined spanwise modes and these modes (and the corresponding feedback loops) are completely altered by the coupling, for the V-shaped configuration. The rest of the paper will focus on this configuration with the exception of a comparison of directivities and broadband shock noise towards the end of the paper.

Fig. 5 shows the tonal frequency characteristics of the single jets when operated separately, and the twin jets in V-shaped configuration, as a function of the fully expanded Mach number. This chart shows that the V-shaped configuration produced screech tones that have a frequency that can be up to about 7% different from the screech tones of either individual jet. An interesting observation is that the frequencies during symmetric mode coupling ($M < 1.4$) are higher than the frequency of either individual jet. In contrast the frequencies during antisymmetric mode coupling are in between (and very close) to that of either jet. Raman and Taghavi [17] showed that such frequency changes during mode jumps are caused by source shifts of the equivalent screech source.

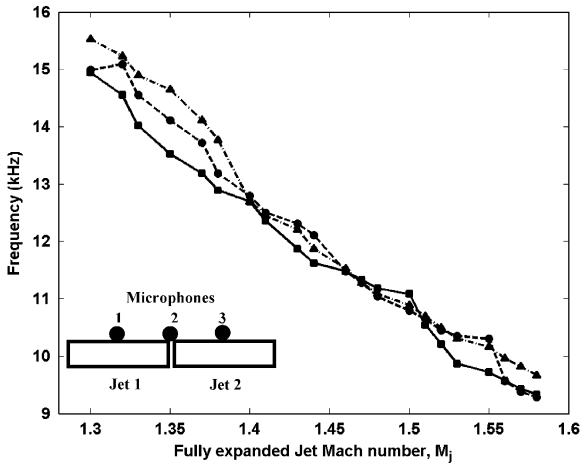

Fig. 5. Frequency characteristics of single beveled nozzles at various fully expanded Mach numbers. The data was taken using microphone 1 for jet 1 operating individually, microphone 3 for jet 2 operating individually and microphone 2 for the twin jet operation. —■—, Jet 1; --●--, Jet 2; –·–▲–·–, twin jet configuration.

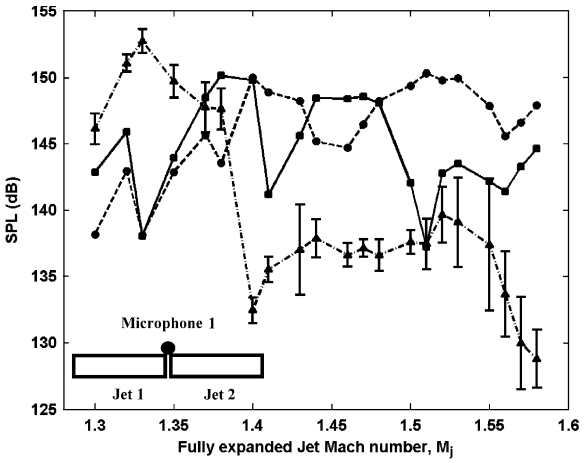

Fig. 6. SPL characteristics of single beveled nozzles at various fully expanded Mach numbers. Note the augmentation in dB levels for the twin jet case at lower M_j and the suppression in the dB levels at medium and high M_j. The data was taken using microphone 1 for all the 3 cases. —■— , Jet 1; ··●··, Jet 2; –·▲·–, twin jet configuration.

Fig. 6 shows the SPL characteristics of single and V-shaped twin jet configurations as a function of the fully expanded jet Mach number. This plot shows the effect of coupling as follows: At the lower Mach numbers, the sound amplitudes for the twin jet are more than 6 dB higher than those of the single jets, that would be expected due to source doubling. An abrupt switch from the symmetric to the antisymmetric coupling occurs at a Mach number of around 1.4, consistent with the phase plot shown in Fig. 4(b). Beyond this Mach number (around 1.4), the twin jet coupling remained antisymmetric for the entire range. Fig. 7 shows a comparative plot of the spectra for the single jet and V-shaped twin jet configuration, for the antisymmetric ($M_j = 1.46$, $s/h = 7.4$), and symmetric ($M_j = 1.33$, $s/h = 7.4$) coupling modes. It is clear from these spectra that coupling renders the peaks sharp, with appreciable amount of power in the fundamental frequency and its harmonics. Non-harmonically related stray peaks observable in single jet spectra get suppressed in the coupling process. For example, many such non-harmonically related peaks can be seen in the spectra of single jets in Figs. 7(a) and (b). These peaks are not observable under coupled conditions.

3.2. Coupling behavior under dynamically varying test conditions

Following static tests, twin jet coupling behavior under dynamically varying test conditions was investigated. Such tests may be relevant to processes occurring during actual flight. However, no attempt is made in the present study to establish a direct correspondence with actual flight operations. The test facilities allowed two parameters to be varied dynamically while the jets operated. They were: (1) the stagnation pressure, and hence the jet Mach number, and (2) the inter-nozzle spacing between the two nozzles. While the former variation was achieved by facility blowdown, thus allowing the stagnation pressure to drop continuously, the latter was possible due to the traversing system used to mount the nozzles, as described in Section 2.

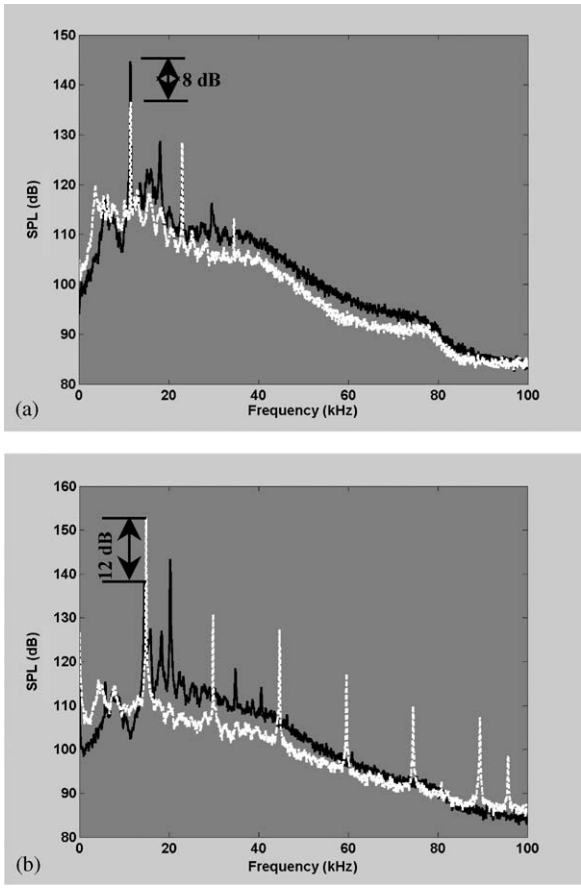

Fig. 7. Spectra illustrating the coupling modes in V-shaped twin jets. (a) Antisymmetric coupling at a fully expanded jet Mach number $M_j = 1.46$. (b) Symmetric coupling at a fully expanded jet Mach number $M_j = 1.33$. Note the difference in amplitude levels for the twin jet case as compared to the individual jets. Black ——, spectra for single jet; white ▪▪▪▪▪, spectra for twin jet configuration.

The blow-down test was performed at a spacing $s/h = 7.4$. While the stagnation pressure dropped, the microphone signals were recorded. The microphones were mounted at the spanwise center of each nozzle. From these signals, spectra and relative phase difference were calculated. Fig. 8 shows spectra for varying Mach number. Fig. 8(a) shows a top view of the three-dimensional spectra shown in Fig. 8(b). While there is a single screech tone at the highest and lowest pressures, intermediate Mach numbers show two dominant non-harmonically related frequencies. The spanwise phase difference between the two microphones at various frequencies and Mach numbers was plotted from which the symmetric and antisymmetric coupling regions were extracted. These iso-phase regions are shown in Fig. 8(c). The frequencies in the phase plot correspond exactly to the tonal frequencies seen in the continuous spectra. This shows the coexistence of symmetric and antisymmetric coupling modes in the V-shaped twin jet under dynamically varying pressure conditions.

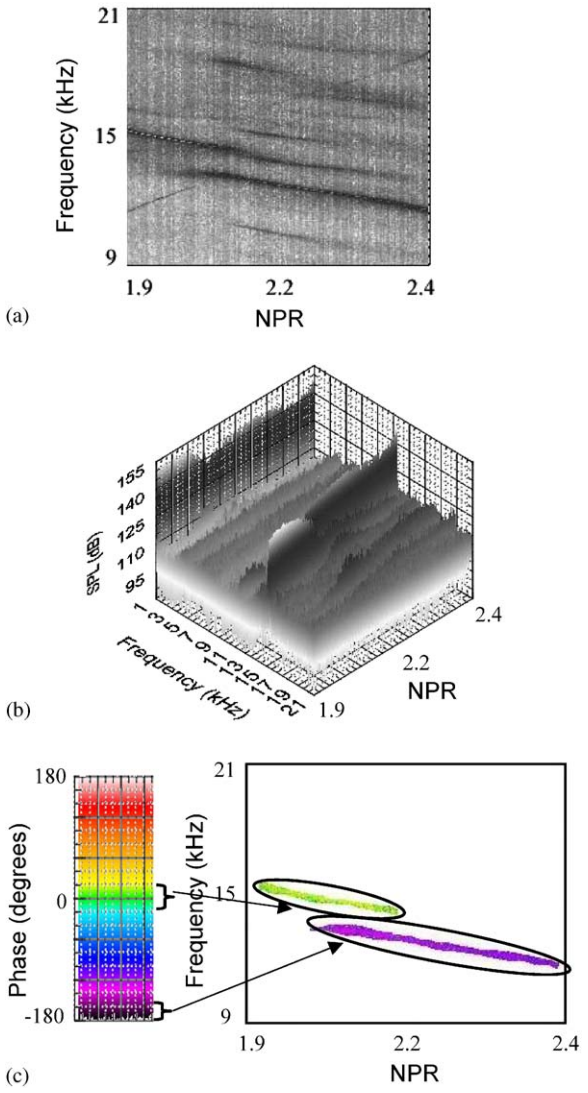

Fig. 8. Continuous instantaneous spectra for nozzles acquired while the inter-nozzle distance remained fixed at $s/h = 7.4$ and the pressure changed continuously. The two modes of coupling can be seen simultaneously at the intermediate pressures at non-harmonically related frequencies. (a) Two-dimensional representation of spectra showing screech frequency variation with change in NPR The plot shows constant SPL contours. (b) Three-dimensional continuous instantaneous spectra. (c) Phase variation with change in the NPR. The shades of gray bar on the left shows the phase variation and the plot on the right shows contours of constant phase.

Continuous spectra were also taken while moving the nozzles apart at a constant rate of 3 mm/s (keeping the pressure constant) in order to check if the jets remained coupled or decoupled. The spectra obtained are shown in Figs. 9(a) and (b). The corresponding phase chart is shown in Fig. 9(c). As can be seen from these two figures, the jets remain coupled in a symmetric mode until around $s/h = 9.7$ after which they start decoupling until eventually no phase locked coupling

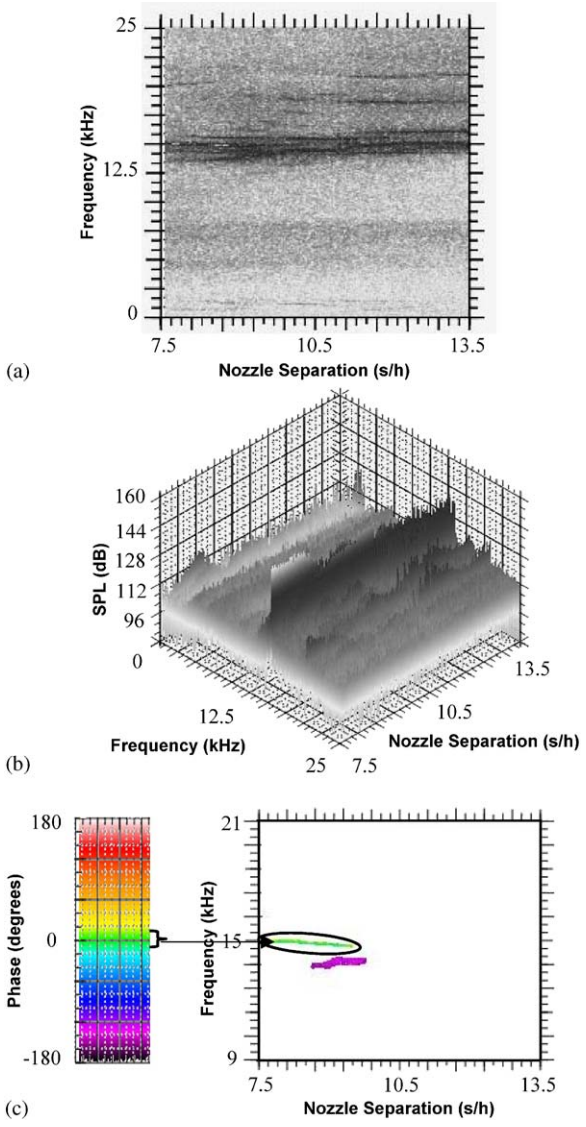

Fig. 9. Continuous instantaneous spectra for nozzles acquired while the inter-nozzle distance changed continuously and the exit jet Mach number remained fixed at 1.33. (a) Two-dimensional representation of spectra showing screech frequency variation with change in the inter-nozzle separation. (b) Three-dimensional continuous instantaneous spectra. (c) Phase variation with change in the nozzle separation. The shades of gray bar on the left shows the phase variation and the plot on the right shows contours of constant phase.

remains at all. Although a strong interaction may be present beyond $s/h = 9.7$, frequency matching between the two jets was no longer observed which contradicts our definition of phase-locked coupling. Note that the time scale at which the nozzles moved apart differed from the time scale of the instabilities in the flow by a factor of 20,000. Clearly, it is not possible to move the nozzles apart at the time scale of instabilities in the flow. Our objective was to acquire data in the

time scale commonly used to deploy nozzle flaps and/or conduct vectoring or aspect ratio change operations on aircraft.

3.3. Nearfield pressure behavior

Since unsteady dynamic pressures could be severe during coupling, it seemed relevant to examine the acoustic pressure distribution in the inter-nozzle region. These nearfield measurements are important to quantify the acoustic loads perceivable by the nozzle structures. The sound pressure was measured by traversing the microphone along the negative X-axis starting at $x/h = 0$ (the point of intersection of the two bevel planes in the V-shaped twin jet) and moving backwards keeping $z/h = 4$ fixed during the test. This study was conducted only for the V-shaped twin jet configuration under coupled and uncoupled conditions (since the A-shaped configuration did not couple). The fully expanded Mach numbers studied were $M_j = 1.33$ and $M_j = 1.46$ for inter-nozzle spacings ratios of $s/h = 7.4$ (where coupling was strongest) and $s/h = 10$ (where coupling was absent as verified from the continuous spectra).

Fig. 10(a) shows the graph comparing the r.m.s. pressure at the various upstream axial locations for $M_j = 1.33$ for the symmetrically coupled case ($s/h = 7.4$) and the uncoupled case ($s/h = 10$). It is clear from this figure that the symmetric coupling produces much higher pressures in the inter-nozzle region when compared to the uncoupled case. Fig. 10(b) shows the same two curves as in Fig. 10(a), along with the addition of the antisymmetrically coupled case at $M_j = 1.46$ ($s/h = 7.4$). It can be seen that when the jets are antisymmetrically coupled the inter-nozzle pressure is lower than that we would see even when the jets are uncoupled. The results show that symmetric coupling produces sound pressures in the inter-nozzle region that are 5.5–7.5 dB higher than those for antisymmetric coupling. Fig. 10(c) adds the curve for the uncoupled case at $M_j = 1.46$ ($s/h = 10$) to the previous figure. This curve shows that this case produces the smallest inter-nozzle pressures. These trends also indicate that inter-nozzle spacing strongly eases the acoustic loading on nearfield structures. For example, in Fig. 10(c), between the two uncoupled cases, the higher Mach number case shows a lower pressure distribution owing to a larger inter-nozzle spacing. Another feature of Figs. 10(a–c) is the fact that the pressures in the inter-nozzle region do not reduce monotonically, rather they exhibit a fluctuating reduction in amplitude. This indicates that the acoustic pressure waves in the upstream inter-nozzle region exhibit a damped standing wave pattern which would explain the continuously reducing oscillatory nature of the pressure amplitude. It must be noted that due to the oscillatory nature, the detrimental effects of the enhanced pressure levels could be felt at far upstream locations in the inter-nozzle region.

Fig. 10(d) shows a comparison between the time series signals for the symmetrically coupled case at $M_j = 1.33$ and the uncoupled case at $M_j = 1.33$ at an upstream location corresponding to $x/h = -3.2$. Similarly, Figs. 10(e) and (f) show comparisons between the time series signals for the symmetrically coupled case at $M_j = 1.33$ and the antisymmetrically coupled case at $M_j = 1.46$, and the symmetrically coupled case at $M_j = 1.33$ and the uncoupled case at $M_j = 1.46$ respectively. In each of these figures, it can be clearly seen that the symmetrically coupled case exhibits regular peaks with greater amplitudes as compared to both the antisymmetric case and the uncoupled case. In addition, the graphs as well as the time series show that the antisymmetric coupling does not automatically imply that the pressure magnitudes are the minimum possible. The minimum possible pressure magnitudes in the inter-nozzle region were obtained when the jets

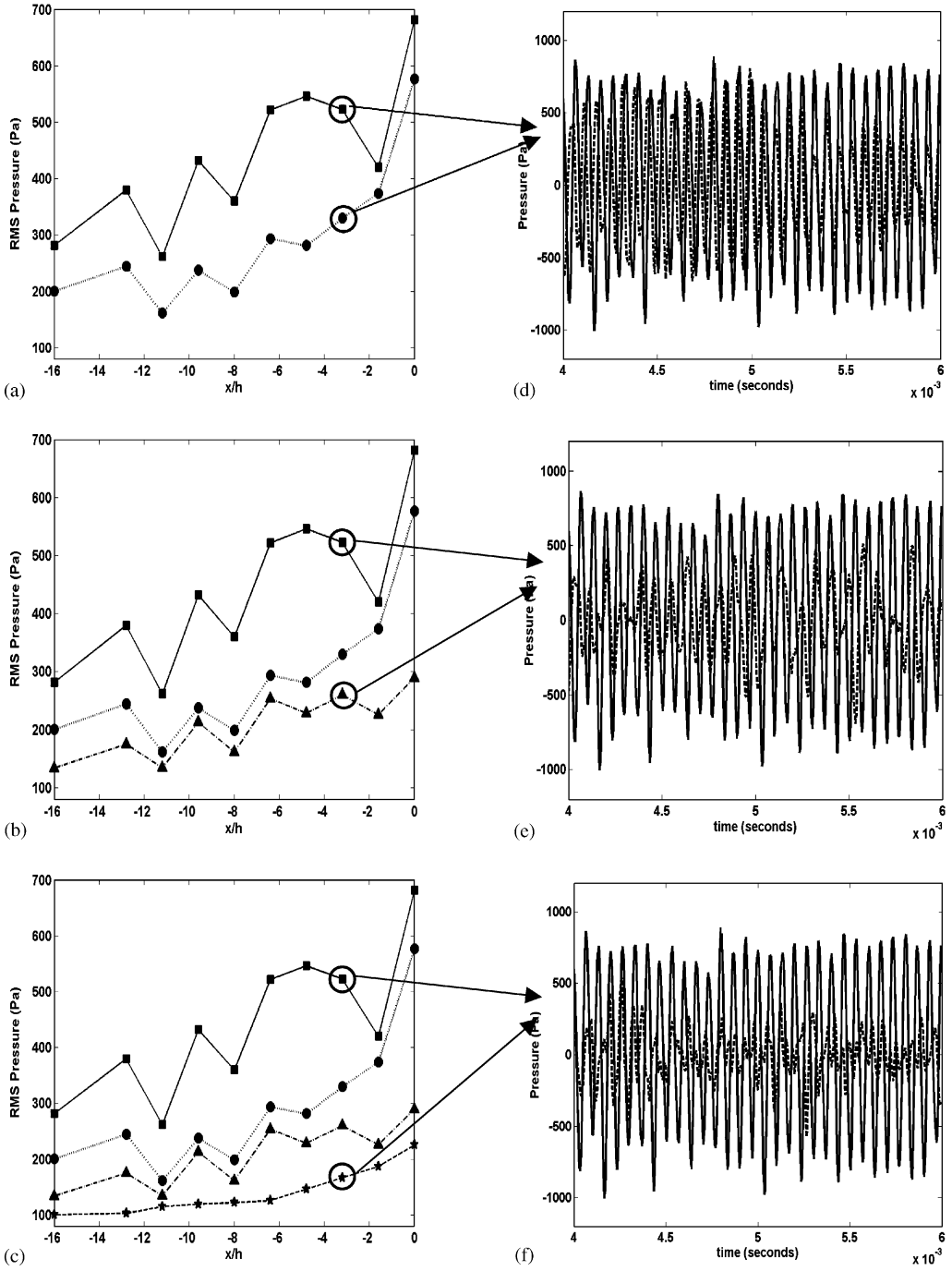

Fig. 10. Inter-nozzle r.m.s. sound pressure distribution. (a–c) Distribution of the r.m.s. pressure in the inter-nozzle region for the various operating conditions. —■—, coupled jets $M_j = 1.33$, ··●··, uncoupled jets $M_j = 1.33$, -·-▲-·-, coupled jets $M_j = 1.46$, ---★---, uncoupled jets $M_j = 1.46$. (d–f) Time series data at the operating conditions circled in the graph. The solid curves (——) are for the coupled case at $M_j = 1.33$ and the dashed curves (– – –) are for the uncoupled case at $M_j = 1.33$; the coupled case at $M_j = 1.46$, and the uncoupled case at $M_j = 1.46$ respectively. Data taken keeping $y/h = 0$ and $z/h = 4$.

were decoupled at Mach numbers that showed antisymmetric coupling at the closest inter-nozzle spacings.

3.4. Phase averaged measurements

In order to obtain the phase averaged readings, the reference microphone was placed in between the two nozzles at the co-ordinate axis origin and the measurement microphone was traversed in the Y direction from a location where $y/h = -10.0$ to $y/h = 10.0$, keeping $x/h = 0.0$ and $z/h = -5.3$ constant. At each measurement location, timeseries data for both the microphones were acquired. The reference signal was digitally filtered around the screech frequency in order to obtain a pure sinusoidal wave. The signal from the measurement microphone at each location was triggered at selected phase angles of the screech cycle from the reference signal. One screech cycle is the time period corresponding to the screech frequency, and was calculated by counting the number of peaks over a certain time period. This was done by the LabVIEW program that performed the phase-averaging. Finally, the sound pressures at the triggered phase angles were ensemble averaged, thus yielding the averaged sound pressure corresponding to that particular phase angle. Fig. 11(a) shows the phase averaged picture along a line on which $x/h = 0$ and $z/h = -5.3$ for an inter-nozzle spacing of $s/h = 7.4$ and a fully expanded jet Mach number of 1.33. In this figure, the curves represent the pressure distribution in the spanwise direction, for a particular position (phase) in the screech cycle. Thus, 24 curves, separated at 15° intervals represent the activity over a cycle (360°) as shown in the figure. For clarity, subsequent curves are translated vertically by 70 Pa. As can be seen from the figure, the pressure magnitudes are symmetric about $y/h = 0$ as expected from a symmetrically coupled jet. Fig. 11(b) shows the phase-averaged picture for a fully expanded jet Mach number of 1.46. As in the previous figure each successive curve corresponds to a 15° increment in phase angle and each curve is offset from the previous by 70 Pa. It can be seen that points on corresponding sides of $y/h = 0$ have pressures that are opposite in phase, revealing antisymmetric coupling. Thus, the coupling modes are documented not only using two point phase measurements but by spatial phase averages that cover the entire spanwise extent of the coupling.

3.5. Applicability of Tam's waveguide approach

A question that naturally arises is: Can we predict or even reconcile the frequencies of complex nozzle coupling that can occur unpredictably in practical situations? To address this question we examined Tam's waveguide mode approach that includes higher order waveguide modes. Tam et. al. [23] showed that the frequencies produced by underexpanded jets of complex geometries could be predicted using a waveguide approach. According to Tam's formula, the predicted frequency is given by

$$f_p = \frac{u_c \kappa}{2\pi\left[1 + u_c/a_\infty\right]}, \tag{1}$$

where u_c is the convection velocity of the instability waves, which, for rectangular jets, was recommended (Tam and Reddy [24]) to be

$$u_c \approx 0.55 u_j, \tag{2}$$

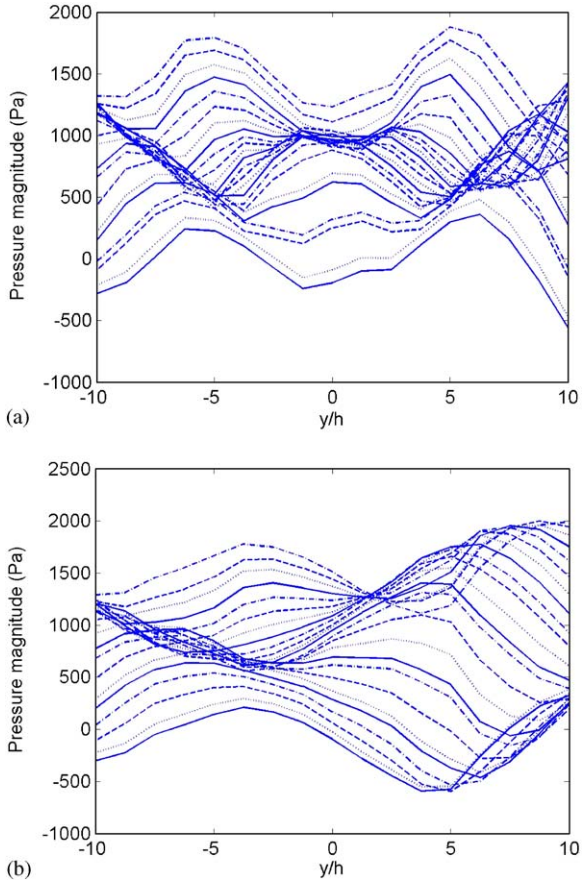

Fig. 11. Phase averaged sound pressure values for the twin nozzles. The values are averaged on either side of the Y-axis keeping the X and Z co-ordinate fixed. (a) Operating condition $M_j = 1.33$. Note the symmetry about $y/h = 0$ indicating symmetric coupling. (b) Operating condition $M_j = 1.46$. Note the antisymmetry about $y/h = 0$ indicating antisymmetric coupling. Successive curves are offset by 70 Pa and a phase difference of 15°. Line codes repeat every 60°.

where u_j is the jet speed, a_∞ is the ambient sound speed, and κ is the wave number of the shock cell structure. Using the vortex sheet model, Tam [25] found out that for large aspect ratio jets, like the ones used in the present study, the value of κ is given by

$$\kappa = k_{n1} = \left(\frac{n^2}{b_j^2} + \frac{1}{h_j^2}\right)^{1/2} \frac{\pi}{(M_j^2 - 1)^{1/2}}, \tag{3}$$

where M_j is the fully expanded jet Mach number. Substituting these values into Eq. (1), the predicted frequency is given by

$$f_p = \frac{0.55u_j}{2\pi[1 + (0.55u_j/a_\infty)]} \left(\frac{n^2}{b_j^2} + \frac{1}{h_j^2}\right)^{1/2} \frac{\pi}{(M_j^2 - 1)^{1/2}}. \tag{4}$$

According to this approach, for rectangular jets with a regular exit geometry, the screech frequency could be accurately predicted using the lowest order waveguide mode, i.e., $n = 1$. In order to test the validity of this approach, we tested two rectangular nozzles with a regular exit geometry in the single jet and twin jet configuration and plotted the screech frequency observed and compared it to Tam's waveguide theory substituting $n = 1$ in Eq. (4). Fig. 12(a) shows the plot for the single and twin jet screech frequencies plotted as a function of the fully expanded jet Mach number. It can be seen from this graph that the observed frequencies show reasonably good agreement with the frequencies corresponding to the lowest order waveguide mode. The observed screech frequencies for the single beveled jets were then plotted as a function of the fully expanded

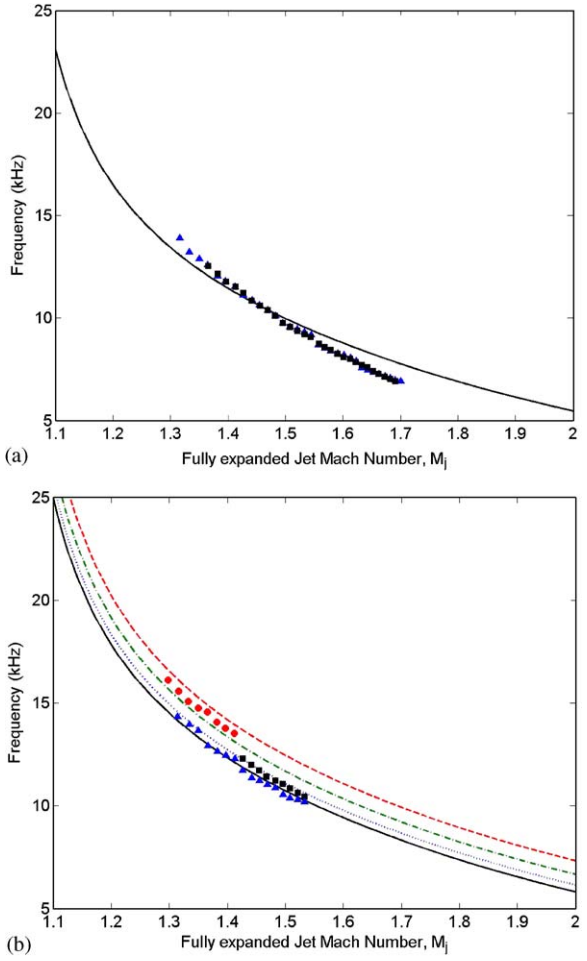

Fig. 12. Screech frequency data compared to Tam's waveguide theory. (a) Screech frequency vs. fully expanded jet Mach number for an aspect ratio 7 rectangular exit jet. ——, Curve for lowest waveguide mode $n = 1$, ▲, single rectangular jet; ■, twin rectangular jets. (b) Screech frequency vs. fully expanded jet Mach number for the single beveled jets used in this study. Curves show waveguide modes: ——, $n = 1$, ▪▪▪▪▪, $n = 2$; —·—·—, $n = 3$; — — —, $n = 4$. ▲, single jet; ●, twin jets symmetrically coupled; ■ twin jets antisymmetrically coupled.

jet Mach number for both the single jet and V-shaped twin jet configurations (Fig. 12(b)). Comparing the observed frequencies with Tam's waveguide modes, we can see that the symmetric coupling case corresponded to a waveguide mode of $n = 3$ and the antisymmetric case corresponded to the modes $n = 2$ and $n = 1$. In contrast the single beveled jet corresponded to an $n = 2$ mode at lower values of the fully expanded jet Mach number and $n = 1$ at the higher values of the fully expanded jet Mach number. However, these predictions strongly depend on the accuracy of the convection velocity used. Since the convection velocity estimate provided by Eq. (2) is for an uniform exit, the extent of validity of this equation for beveled exits needs to be verified by actual measurements of u_c for these jets. Although the waveguide approach cannot provide an a priori estimate of the frequency, the agreement suggests that the tool can indicate to a nozzle designer the range of expected screech frequencies.

Having studied the V-shaped configuration to a certain amount of detail, it was disappointing to note that the A-shaped configuration was not amenable to similar analyses due to the absence of coupling. However, the possibility of looking into the differences between the two configurations is interesting. Among the several possible discrimination tools, directivity measurement was chosen for studying the differences between the two twin jet configurations. These studies are described in the following section.

3.6. Directivity studies

The directivity of sound pressure was measured along the vertical plane (the XZ plane as depicted in Fig. 3(a)) separating the two nozzles. The focus of these studies was to gain knowledge about the differences between the various configurations. Therefore, the directivity was measured for the single jet configuration, the V-shaped twin jet configuration, and the arrowhead-shaped twin jet configuration. The radius of the microphone arc (R) was chosen as 4.5 in (114.3 mm), which corresponds to around 4.5 equivalent diameters, or 22.5 shorter dimensions of the rectangular nozzles, or between 3.5 and 5.3 acoustic wavelengths corresponding to the screech frequency range in the present study. These values are acceptable since the present study focuses on the nearfield effects.

Fig. 13 shows the comparison between the two twin jet configurations (arrowhead-shaped, and V-shaped). In both the cases, the s/h was fixed at 7.4, and the Mach number was maintained at 1.33. The V-shaped configuration coupled symmetrically, and the arrowhead configuration did not show coupling at these conditions. The spectra of these two configurations can be distinguished by the fact that the symmetrically coupled V-configuration shows sharp tones of significant intensities against the multi-peak spectra of the uncoupled arrowhead configuration jets. In the case of the arrowhead configuration, the rise in the screech amplitude with increasing angle is also accompanied by an increase in the broadband shock noise. However, in the case of the symmetrically coupled V-shaped jet, there is no observable increase in the broadband shock associated noise. It may also be seen from the figures that the spectra of the arrowhead configuration are more sensitive to the emission angle as in single jets. This can be reconciled from the fact that when two jets do not couple, their sensitivity to angle remains unaltered.

Fig. 14 shows the comparison of spectra of the arrowhead and V-shaped twin jets at various emission angles of measurement in the vertical plane. The jets were operated at a higher Mach

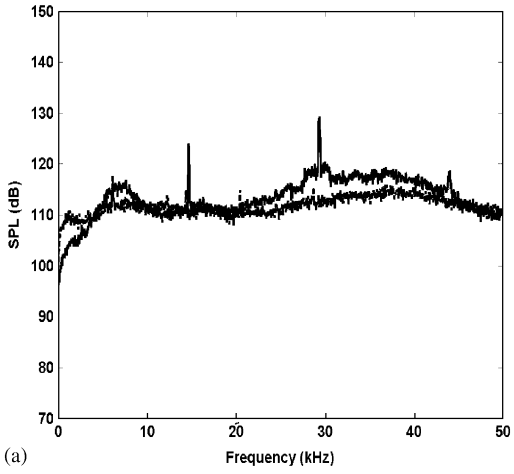
SPL (dB)
Frequency (kHz)

(a)

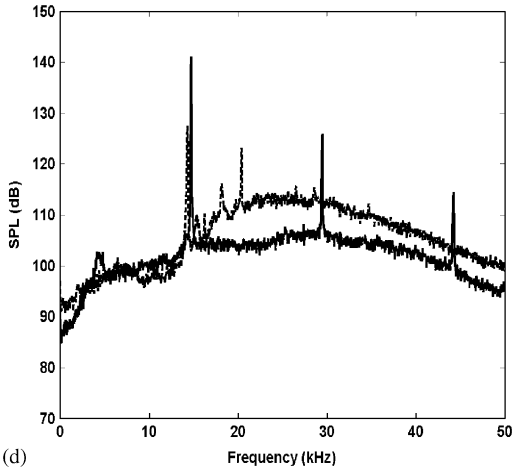
SPL (dB)
Frequency (kHz)

(d)

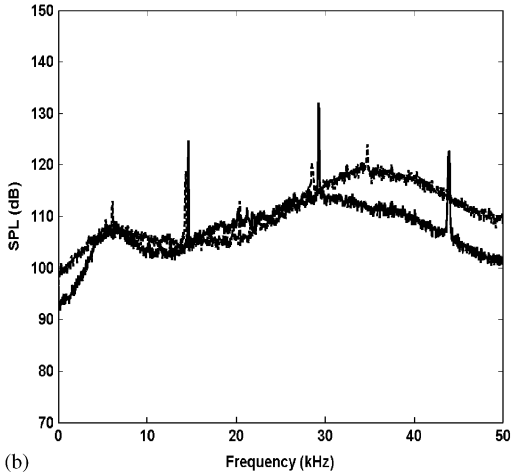
SPL (dB)
Frequency (kHz)

(b)

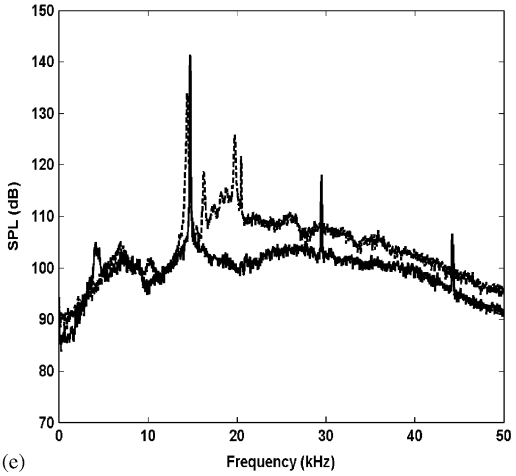
SPL (dB)
Frequency (kHz)

(e)

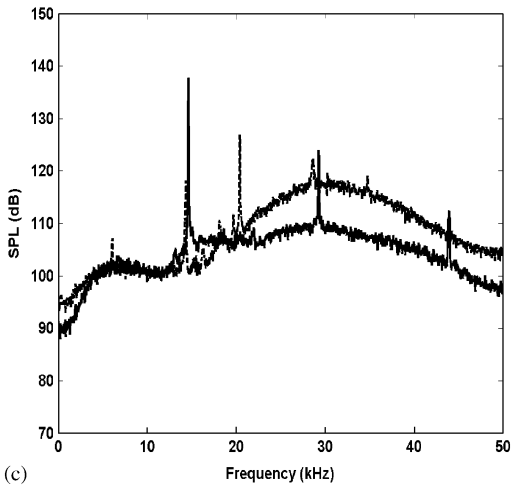
SPL (dB)
Frequency (kHz)

(c)

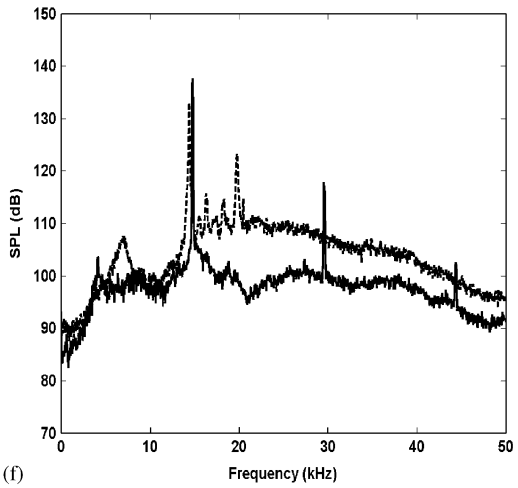
SPL (dB)
Frequency (kHz)

(f)

number of 1.46, at which the V-shaped twin jet coupled anti-symmetrically, as discussed earlier. The following may be observed from these spectra:

(1) Antisymmetric coupling (V-shaped jets) shows significantly lower amplitudes than arrowhead configuration at all angles.
(2) Antisymmetric coupling (V-shaped jets) shows more broadband noise than symmetric coupling (V-shape).

3.7. Broadband shock noise

In order to compare the broadband shock associated noise from each configuration, it was necessary to define an invariant metric to quantify this noise, that was applicable to all the cases compared. This was achieved using the NASA preferred reliability practice no. PD-ED-1259. A constant bandwidth of 10 kHz was used in each spectra, where the most dominant broadband noise occurred at frequencies higher than the fundamental screech frequency. Further, it was ensured that this band excluded any tones or harmonics. Then, the integrated SPL over this band was calculated. As in the previous Section 3.6, comparisons have been made for single and the two configurations of the twin jets.

The broadband noise content of the single jet and the twin jets in the V-shaped and the arrowhead configurations are compared in Fig. 15. These plots are for the higher Mach number case ($M_j = 1.46$) where the broadband noise predominates. From Fig. 15, it can be seen that the broadband noise of the twin jets is far greater than that of a single jet. It is to be noted that the V-shaped twin jet configuration corresponds to the antisymmetric coupling, which showed more than the 6 dB lower SPL at the screech tone. Thus, it is clear that a reduction in the tonal amplitude due to the antisymmetric coupling mode does not imply reduced levels in other noise components, an observation that has hitherto gone unreported in the twin jet literature. Thus, coupling should be understood to have a pronounced effect only with respect to screech frequencies and their harmonics. Similarly, a comparison of the broadband shock noise of the V-shaped and arrowhead-shaped twin jet configurations at $M_j = 1.46$ shows that the V-shaped twin jet configuration, that is much noisier than a single jet, was found quieter in comparison with the arrowhead-shaped twin jet configuration. This indicates the possibility that there is a strong interrelationship between the two shock-cells from the two individual jets in the case of coupled twin jets. This would imply that in cases where this interaction between shock-cells is inhibited, as in the case of the arrowhead shape, the two sets of shock cells would act independently, leading to a behavior consistent with the following observations made in the present study:

(1) Individual jets screech at different frequencies.
(2) Shock-associated noise increases with change in configuration from V to A, for the same pressure, mass flow rate and momentum.

Fig. 13. Comparison between twin jet spectra for various angles at an arc radius of $r/h = 22.5$ in the vertical plane XZ plane depicted in Fig. 3a for the arrowhead and the V-shaped configurations at $M_j = 1.33$ at $s/h = 7.4$: (a) 50°, (b) 70°, (c) 90°, (d) 110° (e) 130°, (f) 150°. Solid curves (——) are for the 'V'-shaped configuration and the dashed curves (– – –) are for the Arrowhead configuration.

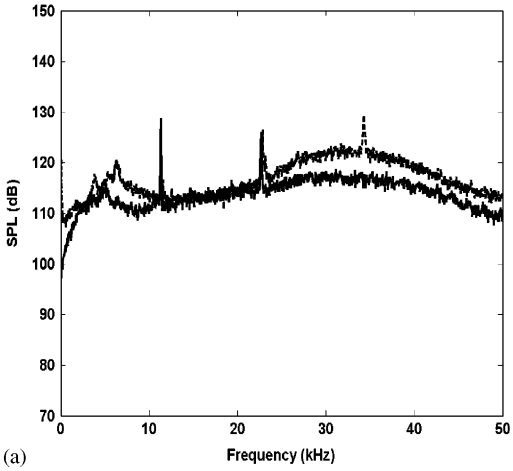
SPL (dB)
Frequency (kHz)

(a)

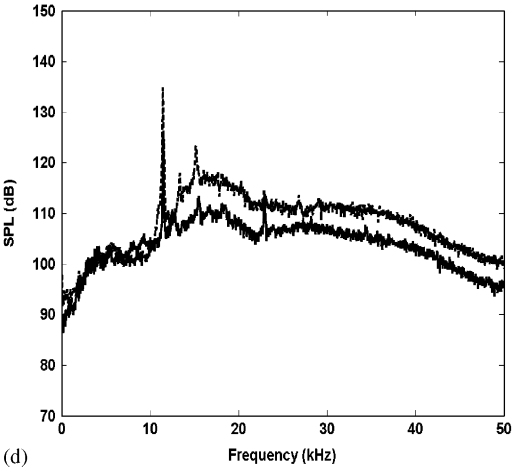
SPL (dB)
Frequency (kHz)

(d)

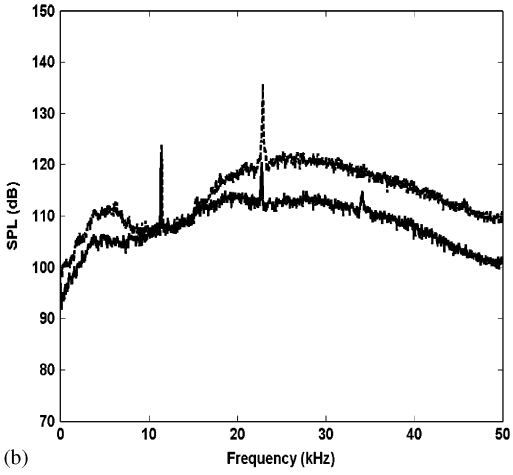
SPL (dB)
Frequency (kHz)

(b)

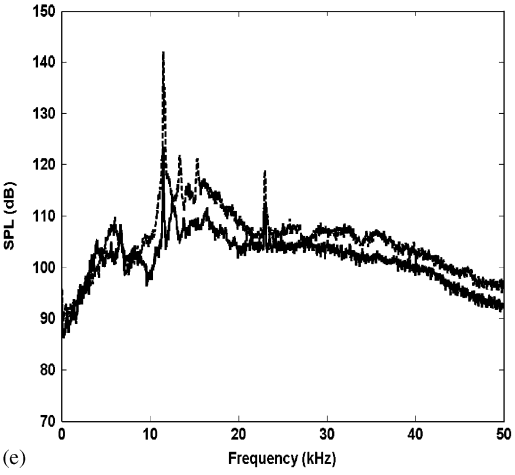
SPL (dB)
Frequency (kHz)

(e)

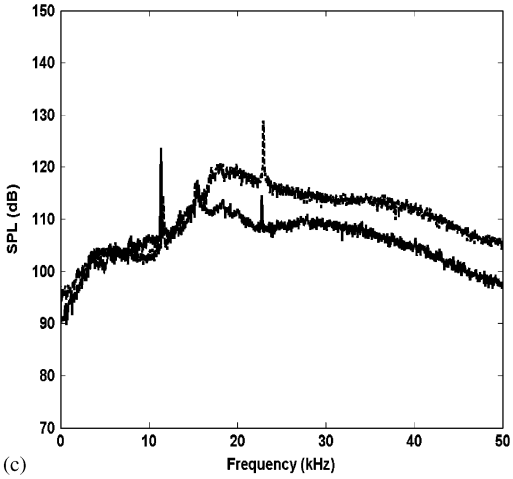
SPL (dB)
Frequency (kHz)

(c)

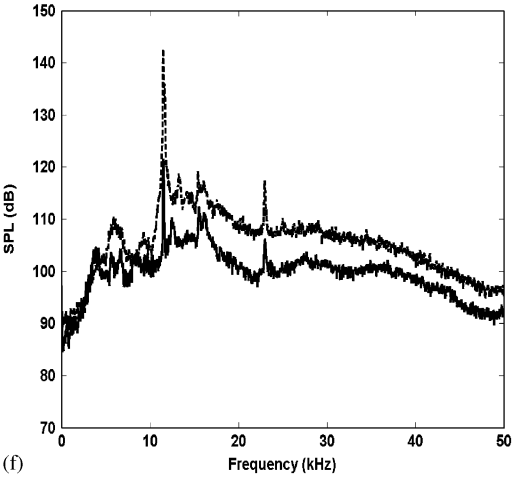
SPL (dB)
Frequency (kHz)

(f)

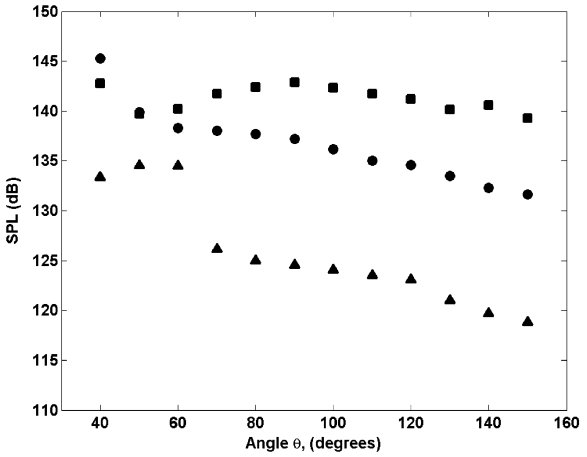

Fig. 15. Broadband shock noise characteristics of single and twin jets at $M_j = 1.46$, $s/h = 7.4$, and at an arc radius of $r/h = 22.5$. ▲, Single jet, ●, twin jets in the V-shaped configuration, and ■, twin jets in the arrowhead configuration. θ is the angle measured with respect to the jet exit axis on the XZ plane depicted in Fig. 3a.

In summary, the broadband shock noise levels for the three configurations studied compare as follows: single jet < V-shaped < arrowhead-shaped. This strongly suggests that there could be contrasting differences in shock structures in the three configurations, which could in turn strongly influence their broadband noise emission behavior.

4. Conclusions

The coupling phenomenon for jets exhausting from twin jets of single beveled geometry has been studied. Two possible twin jet configurations, namely the arrowhead-shaped configuration and V-shaped configuration were compared. Studies focused at the closest spacing and dynamic tests were conducted at higher inter-nozzle spacings. Key results are summarized below:

1. We were able to demonstrate coupling between twin supersonic jets exhausting from nozzles of single beveled geometry. For the nearest inter-nozzle spacing ($s/h = 7.4$), the V-shaped twin jets coupled in a symmetric mode at the lower Mach numbers and in an antisymmetric mode at the higher Mach numbers. In contrast, the arrowhead (A-shaped) configuration did not show coupling at all spacings and Mach numbers covered in this study.
2. The symmetric coupling produced higher tonal peaks than those produced by single jets and the antisymmetric coupling lead to a reduction in the tonal peaks as compared to single jets. The augmentation and the reduction were both greater than the 6 dB that we would expect through

Fig. 14. Comparison between twin jet spectra for various angles at an arc radius of $r/h = 22.5$ in the vertical plane XZ plane depicted in Fig. 3a for the arrowhead and the V-shaped configurations at $M_j = 1.46$ at $s/h = 7.4$: (a) 50°, (b) 70°, (c) 90°, (d) 110°, (e) 130°, (f) 150°. Solid curves (——) are for the 'V'-shaped configuration and dashed curves (– – –) are for the arrowhead configuration.

source doubling/halving for tones. Phase averaged measurements in the near field confirmed symmetric coupling in the case of $M_j = 1.33$ and antisymmetric coupling at $M_j = 1.46$.

3. Dynamic tests conducted for the nozzles at their closest inter-nozzle spacing showed the existence of both coupling modes at non-harmonically related frequencies for the midrange of pressures tested. The dynamic spectra acquired by moving the nozzles apart while running the jets at a fully expanded Mach number of 1.33 showed that the nozzles coupled in a symmetric mode until about $s/h = 9.7$. After this they decoupled and no further phase locked coupling was seen.
4. The measured screech frequencies agreed well with the waveguide modes proposed by Tam et al. [23]. The screech frequencies of the symmetrically coupled V-shaped twin jet corresponded to the higher order waveguide modes ($n = 3$), while those of antisymmetric coupling corresponded to modes between $n = 1$ or $n = 2$.
5. Coupled jets had the same fundamental frequencies and harmonics dominant at all emission angles, while the spectra were sensitive to direction for single and uncoupled (A-shaped) twin jets.
6. The broadband shock associated noise had a strong dependence on the configuration, and hence possibly the shock-structures and their inter-relationships. Studies at Mach 1.46 revealed that the coupled twin jet in V-configuration emitted lower broadband shock noise followed by the uncoupled twin jet in the A-configuration.

Our detailed studies have demonstrated the possibility of achieving significant change in the acoustic behavior through a simple configuration change. We expect our findings to be useful for both nozzle designers and those developing numerical models for multi-nozzle configurations.

Acknowledgements

This work was funded by the US Air Force Office of Scientific Research (AFOSR) with Dr. Steven Walker and Dr. John Schmisseur as Program Managers.

References

[1] A. Powell, On the mechanism of choked jet noise, *Proceedings of the Physical Society of London* B66 (1953) 1039–1056.
[2] G. Raman, Supersonic jet screech: half-century from Powell to the present, *Journal of Sound and Vibration* 225 (1999) 543–571.
[3] D.E. Berndt, Dynamic pressure fluctuations in the internozzle region of a twin-jet nacelle, SAE-841540, Society of Automotive Engineers, Warrendale, PA, Oct. 1984.
[4] J.M. Seiner, J.C. Manning, M.K. Ponton, Dynamic pressure loads associated with twin supersonic plume resonance, *American Institute of Aeronautics and Astronautics Journal* 26 (1988) 954–960.
[5] C.K.W. Tam, J.M. Seiner, Analysis of twin supersonic plume resonance, American Institute of Aeronautics and Astronautics Paper 87-2695, 1987.
[6] P.J. Morris, Instability waves in twin supersonic jets, *Journal of Fluid Mechanics* 220 (1990) 293–307.
[7] R.W. Wlezien, Nozzle geometry effects on supersonic jet interaction, American Institute of Aeronautics and Astronautics Paper 87-2694, 1987.

[8] L. Shaw, Twin-jet screech suppression, *Journal of Aircraft* 27 (8) (1990) 708–715.
[9] J.S. Lilley, The design and optimization of propulsion systems employing scarfed nozzles, *Journal of Spacecraft and Rockets* 23 (1986) 597.
[10] R.W. Wlezien, V. Kibens, Influence of nozzle asymmetry on supersonic jets, *American Institute of Aeronautics and Astronautics Journal* 26 (1988) 27.
[11] E.J. Rice, G. Raman, Mixing noise reduction for rectangular supersonic jets by nozzle shaping and induced screech mixing, American Institute of Aeronautics and Astronautics Paper 93-4322, 1993; National Aeronautics and Space Administration Technical Memorandum 106364, 1993.
[12] E.J. Rice, G. Raman, Supersonic jets from bevelled rectangular nozzles, American Society of Mechanical Engineers Paper No. 93-WA/NCA-26, 1993; National Aeronautics and Space Administration Technical Memorandum 106403, 1993.
[13] E.J. Rice, Jet mixer noise suppressor using acoustic feedback, United States Patents 5,325,661 and 5,392,597, 1995.
[14] J.-H. Kim, M. Samimy, On mixing enhancement via nozzle trailing edge modifications in high speed jets, *American Institute of Aeronautics and Astronautics Journal* 38 (5) (2000) 935–937.
[15] C. Kerachanin, M. Samimy, J-H. Kim, Effects of nozzle trailing edges on acoustic field of a supersonic rectangular jet, *American Institute of Aeronautics and Astronautics Journal* 39 (6) (2001) 1065–1070.
[16] G. Raman, R.R. Taghavi, Resonant interaction of a linear array of supersonic rectangular jets: an experimental study, *Journal of Fluid Mechanics* 309 (1996) 93–111.
[17] G. Raman, R. Taghavi, Coupling of twin rectangular supersonic jets, *Journal of Fluid Mechanics* 354 (1998) 123–146.
[18] R.R. Taghavi, G. Raman, Interaction of twin rectangular supersonic jets in various configurations, American Society of Mechanical Engineers Fluids Engineering Division Summer Meeting, Washington, DC, FEDSM98-5243, 1998.
[19] G. Raman, Coupling of twin supersonic jets of complex geometry, *Journal of Aircraft* 36 (5) (1999) 743–749.
[20] G. Raman, Screech tones from rectangular nozzles with spanwise oblique shock-cell structures, *Journal of Fluid Mechanics* 330 (1997) 141.
[21] G. Raman, Shock-induced flow resonance in supersonic jets of complex geometry, *Physics of Fluids* 11 (3) (1999) 692–709.
[22] D.E. Zilz, R.W. Wlezien, The sensitivity of near-field acoustics to the orientation of twin two-dimensional supersonic nozzles, American Institute of Aeronautics and Astronautics Paper 90-2149, 1990.
[23] C.K.W. Tam, H. Shen, G. Raman, Screech tones of supersonic jets from beveled rectangular nozzles, American Institute of Aeronautics and Astronautics Paper 97-0143, 1997.
[24] C.K.W. Tam, N.N. Reddy, Prediction method for broadband shock associated noise from supersonic rectangular noise, *Journal of Aircraft* 33 (2) (1996) 298–303.
[25] C.K.W. Tam, The shock-cell structure and screech tone frequencies of rectangular and non-axisymmetric supersonic jets, *Journal of Sound and Vibration* 121 (1988) 135–147.